Structural Engineering and Mechanics, Vol. 45, No.6 (2013) 723-740
DOI: http://dx.doi.org/10.12989/sem.2013.45.6.723

A parametric study of optimum tall piers for railway bridge viaducts

Francisco J. Martínez-Martín[1a], Fernando González-Vidosa[2b], Antonio Hospitaler[2c] and Víctor Yepes[*2]

[1]Department of Geotechnical Engineering, Universitat Politècnica de València, Camino de Vera s/n, 46022 Valencia, Spain
[2]Department of Construction Engineering, Institute of Concrete Science and Technology (ICITECH), Universitat Politècnica de València, Camino de Vera s/n, 46022 Valencia, Spain

(Received December 7, 2011, Revised February 1, 2013, Accepted February 19, 2013)

Abstract. This paper presents a parametric study of reinforced concrete bridge tall piers with hollow, rectangular sections. Such piers are typically used in railway construction of prestressed concrete viaducts. Twenty one different piers have been studied with seven column heights of 40, 50, 60, 70, 80, 90 and 100 m and three types of 10-span continuous viaducts, whose main span lengths are 40, 50 and 60 m. The piers studied are intermediate columns placed in the middle of the viaducts. The total number of optimization design variables varies from 139 for piers with column height of 40 m to 307 for piers with column height of 100 m. Further, the results presented are of much value for the preliminary design of the piers of prestressed concrete viaducts of high speed railway lines.

Keywords: ant colony optimization; concrete structures; economic optimization; structural design; tall piers

1. Introduction

The initial step in the design of railway viaducts is deciding the position and total length of the bridge (see Fig. 1). It then follows the adoption of the number of bays and its main span length. The height of the valley is a key aspect on this decision. It is common sense that high valleys require tall piers and large span lengths. On the other hand, low valleys require short piers and shorter span lengths. Hence, the design of a viaduct requires either the adoption of more piers with smaller span lengths or less piers with larger span lengths. The design of bridge piers is therefore essential for the design of prestressed concrete viaducts, since piers make up to 50% of the total cost of the viaduct depending on pier heights and foundation conditions. Piers are usually considered tall when the height of the shaft is larger than 50 m, while shorter than 50 m height

∗Corresponding author, Associate Professor, E-mail: vyepesp@cst.upv.es
[a]Assistant Professor, E-mail: framarm1@upv.es
[b]Professor, E-mail: fgonzale@upv.es
[c]Professor, E-mail: ahospitaler@upv.es

piers are generally considered not high enough to be considered tall piers. Short piers do not generally require inclined walls, whereas tall piers need variable cross-section walls due to the great variation of efforts along the shaft. The construction procedure of tall piers is easier when only two walls along the shaft are inclined. On the other hand, should the four walls be inclined, it is then necessary to descend to the ground the internal formwork in order to change its size. All this causes extra work and machinery, which raises the production cost with respect to the constant or two inclined walls cross-sections. Regarding the geometry of the cross-section, rectangular hollow sections are most frequently used for tall piers. In fact, a large number of reinforced concrete (RC) bridges constructed in Europe between 1950s and 1970s are characterized by hollow-core piers (Lignola *et al*. 2007).

A pier behaves like a loaded cantilever beam (Fig. 2). Hollow-core piers are often used where tall piers are required. Their beneficial characteristics, compared to solid piers, provide a considerable reduction in the volume of the concrete, large reduction in weight (consequently can reduce the inertial seismic force), and high bending and torsion stiffness. In addition, the high radius of gyration of rectangular hollow sections improves the strength against instability due to second-order effects. In this context, structural optimization of this type of large and repetitive structures is an area of much research interest given the large amount of materials required in the construction procedure.

During the last 50 years, structural optimization problems have been extensively studied and published (Adeli and Sarma 2006). The breakthrough of personal computing around 1980 became a starting point for the structural analysis development, especially as regards the use of finite elements-based models. Other advances in the 1990s came with the use of the computer-aided design (CAD) tools, which significantly improved the process of structural design. Up to very recently, those design tools did not, by themselves, optimize any structure, since structures were designed based on data supplied by users. The only way to improve the CAD designs was to make several tests and reject those solutions that did not fulfill any requirements imposed by the designer, on a trial-and-error basis, where human-computer interaction is essential. Fortunately, optimization methods have provided an effective alternative to traditional-based design methods, CAD-based software inclusive. However, strong emphasis on the value of the designer's experience, whose good judgment is essential to decide, ultimately, any suggested computer design, should be highlighted. In contrast to designs based on experience, artificial intelligence has dealt since its appearance with a variety of fields that include the solution of constrained problems.

Emergence of heuristic optimization techniques was a consequence of artificial intelligence procedures. These approximate techniques are appropriate for optimizing realistic structures because they often find a fast and near global optimal solution. Heuristic approaches include

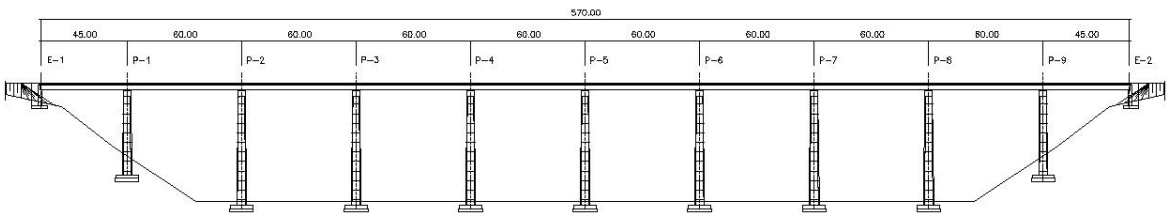

Fig. 1 Typical elevation of a prestressed concrete railway viaduct

several algorithms such as genetic algorithms (Holland 1975), simulated annealing (Kirkpatrick *et al*. 1983), particle swarm optimization (Kennedy and Eberhart 1995), ant colony optimization (Dorigo *et al*. 1996), and harmony search optimization (Lee and Geem 2004), inter alia. A recent review of metaheuristics for project and construction management can be found in the study by Liao *et al*. (2011).

Cohn and Dinovitzer (1994) provided an extensive state-of-the-practice in structural optimization; in this study, they brought out the gap between theoretical aspects and practical problems of structural optimization, adding that mathematical optimization represents a high degree of complexity for the structural engineer and noting that most of the research studies focused mainly on steel structures, whereas only few dealt with concrete structures. Size, topology, and geometry structural optimization has been carried out in the last three decades (Martínez *et al*. 2007). Recently, genetic algorithms have been applied to structural design optimization, such as glass fibre reinforced polymer bridge deck (Lee and Park 2011), and fibre composite railway sleeper (Awad and Yusaf 2012).

The history of heuristic optimization in RC structures can be traced back to the late 1990s (Balling and Yao 1997, Coello *et al*. 1997). From them on, many studies based on evolutionary computation have been applied for optimizing structural concrete problems, especially genetic algorithms. Kicinger *et al*. (2005) provided a review of evolutionary algorithms and structural

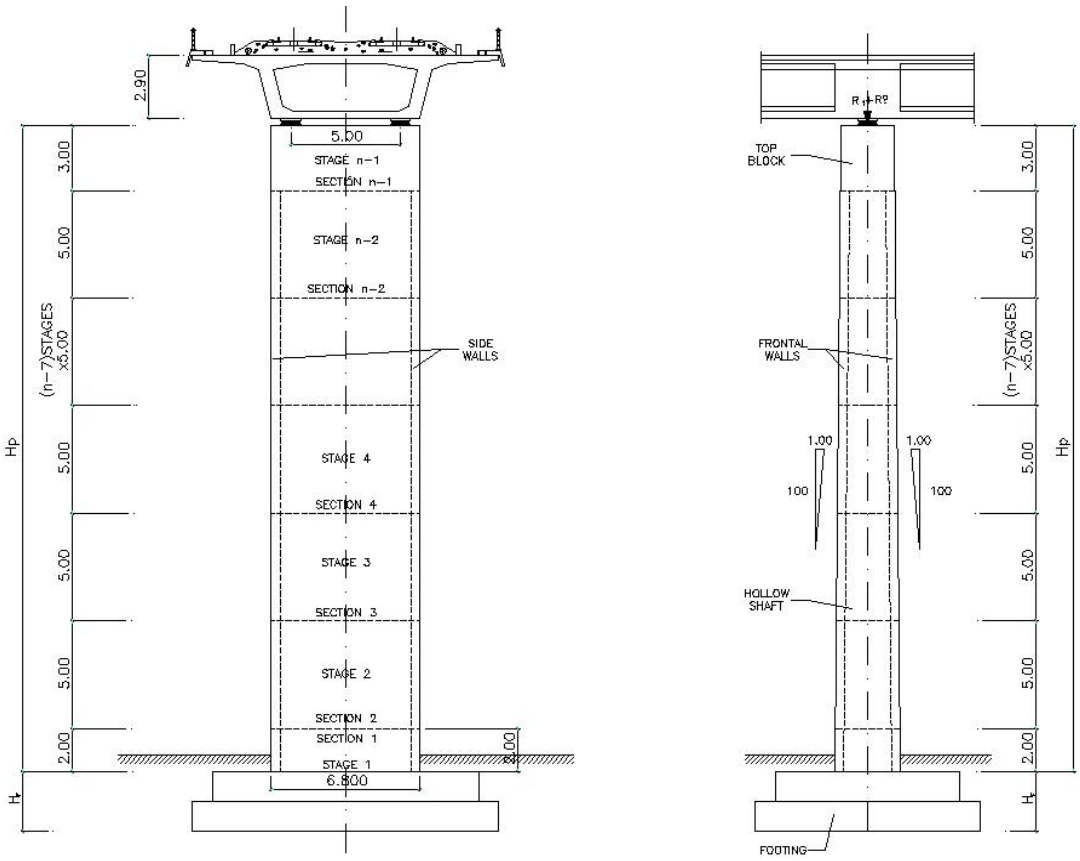

Fig. 2 Typical frontal and side elevations of a bridge pier

design. However, several studies have been undertaken in recent years to implement other algoritms to solve RC problems such as simulated annealing, particle swarm optimization, ant colony optimization, harmony search and big bang-big crunch heuristic (Li *et al*. 2010, Kaveh and Sabzi 2011, Khajehzadeh *et al*. 2011). The present authors' research group has recently reported on non-evolutionary algorithms to the fully automated structural design and cost optimization of realistic three-dimensional structures such as walls (Yepes *et al*. 2008, 2012), frame bridges (Perea *et al*. 2008, 2010), building frames (Payá *et al*. 2008, Payá-Zaforteza *et al*. 2009, 2010), bridge piers (Martínez *et al*. 2010, 2011), prestressed concrete precast road bridges (Martí *et al*. 2013), and road vaults (Carbonell *et al*. 2011).

A model for the optimal design of hollow, rectangular RC bridge piers was developed in previous works (Martínez *et al*. 2010, 2011), which described the optimization model in terms of the design variables, the cost function, the analysis parameters, the structural constrains and the optimization methodology based on population algorithms such as the ant colony and genetic algorithms, together with neighbourhood-based algorithms such as the simulated annealing and a threshold accepting algorithms. Once the model is studied and calibrated, it is used as the basis for the parametric study presented in this article. Hence, while the initial publications concentrated on the development of an automatic design model for high and tall piers, the present publication concentrates on the analysis and design of optimum tall piers with different heights and for different span lengths for railway bridges. The present publication aims to guide designers as to the characteristics of optimum designs for railway viaducts, and thus reduce the time needed for preliminary designs of bridge piers.

2. Optimum design problem

2.1 Piers object of optimization

The rectangular hollow-core section piers object of this study are those commonly used in the construction of cast-in-place prestressed concrete railway viaducts. Seven different vertical pier heights of 40, 50, 60, 70, 80, 90 and 100 meters were considered. Regarding the viaduct type, three typical viaducts of 10 continuous bays with main span length of 40, 50 and 60 m were considered, i.e., viaducts of 30-8x40-30 m, 37.50-8x50-37.50 m and 45-8x60-45 m. Hence, a total of 21 piers were analyzed. The parts of the hollow rectangular pier are the following (Fig. 2): the foundation that is either a surface footing or can include deep piles, the main hollow shaft and the solid top part that sustains the reactions of the pair of pot bearings of the bridge deck. The construction is normally done in column stages of about 5.00 m in height. The height of the end top part is 3.00 m. Consequently, the piers are built in stages; every stage is limited by two sections, so the number of sections and stages of the piers depend on their height (Table 1). The dimensions of the footing are proportioned in such a way that the maximum pressure does not exceed the permissible ground stress. Alternatively, a piled foundation is required when there is not enough ground strength. The main parameters that affect pier design are the pier height as well as the vertical and horizontal loads that transfer the deck and the allowable soil pressure. Loads and external influences to which a bridge is subjected in the structural analysis used in this study are defined in the Spanish IAPF-07 code for actions and design requirements of railways bridges (Ministerio de Fomento 2007) and at a European level in EN 1991-2: Eurocode 1 (CEN 2003). The EN 1998-1: Eurocode 8 (CEN 2004b) provisions need not be observed due to the very low seismicity considered in this study. A

previous step in the verification of limit states consists of the calculation of stress envelopes due to actions. As regards actions, gravity actions include self-weight and non-structural dead loads. Variable actions include the traffic and wind loads according to IAPF-07 and EN1991-2. A longitudinal friction force is transmitted by the pot bearings to the pier. The wind load is considered with calculation velocity equal to 28 m/s. The load combination factor depends upon the limit state considered. Once the stress resultants are known, it follows checking all the serviceability and ultimate limit states prescribed by concrete codes: EHE (Ministerio de Fomento 2008) and EN 1992-1-1: Eurocode 2 (CEN 2004a). The deck cross-sections considered are depicted in Figs. 3 to 5. The width of the platform is 14.00m in all cases. As shown in these Figures, this width can accommodate a two-way line and maintenance pathways. The 40-50-60-m span viaducts considered have a depth of 2.30-2.90-3.45m. The soffits of the cross-sections have been kept constant to 6.80m, which coincides with the transverse dimension of all piers studied, i.e., the transverse dimension of the piers is a parameter which does not vary throughout the whole study, while the longitudinal dimension of the pier varies for each optimum pier. The dimensions of the deck cross-sections have been chosen following the authors' experience on this type of viaducts.

2.2 Problem statement

The aim herein is to design a hollow, rectangular RC bridge pier that minimizes the structural cost F in Eq. (1) and Section 2.3. The study aims to minimize the labor and material cost while meeting building code requirements for safety and serviceability structural constraints in Eq. (2) and Section 2.4 of the problem.

$$F(x_1, x_2, ..., x_n) = \sum_{i=1,r} p_i * m_i(x_1, x_2, ..., x_n) \tag{1}$$

$$g_j(x_1, x_2, ..., x_n) \le 0 \tag{2}$$

$$x_i \in (d_{i1}, d_{i2}, ..., d_{iq}) \tag{3}$$

Note that the cost function is the sum of unit prices (p_i) multiplied by the measurements of construction units (m_i) (formwork, concrete, steel, etc). Moreover, the structural constrains are all the serviceability limit states (SLSs) and ultimate limit states (ULSs) that must be met by the structure, as well as the geometric, constructability and durability constraints of the problem. Besides that x_1, x_2,..., x_n are the design variable for the analysis that can take the discrete values in a list in Eq. (3).

Table 1 Number of sections and stages of the columns

Column height (m)	Sections	Stages
40	10	9
50	12	11
60	14	13
70	16	15
80	18	17
90	20	19
100	22	21

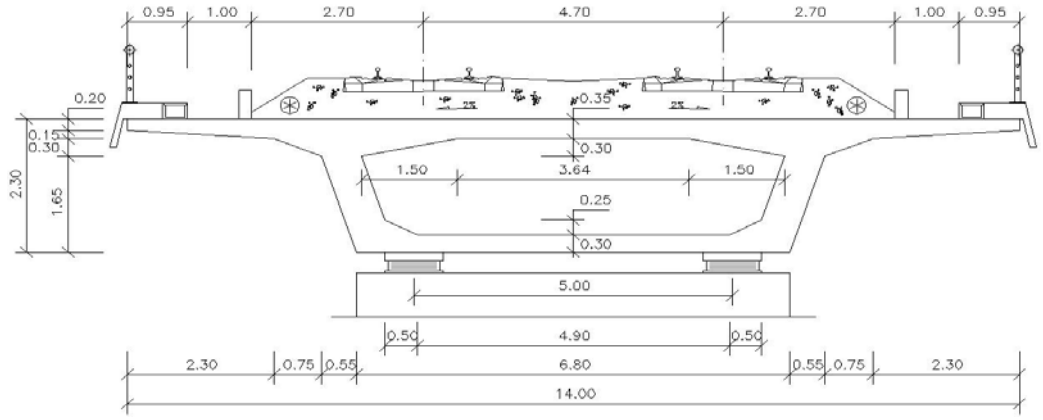

Fig. 3 Deck-section considered for the 40 m span railway viaducts

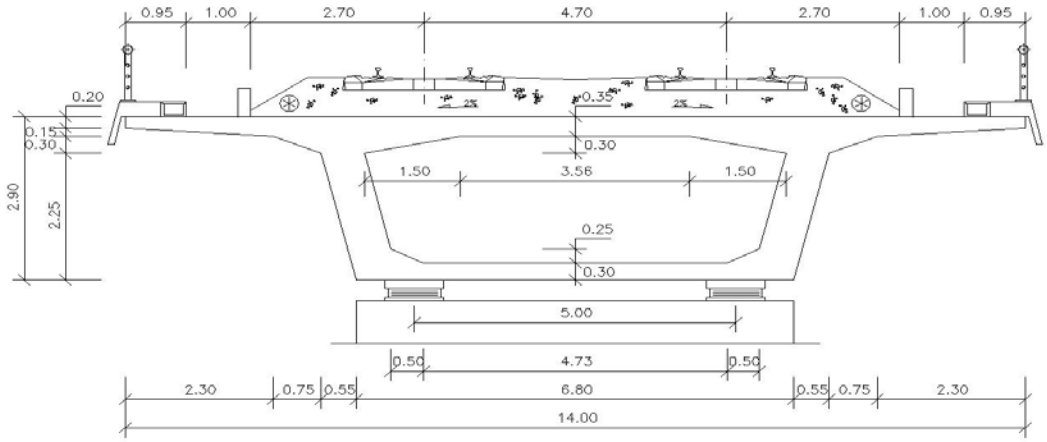

Fig. 4 Deck-section considered for the 50 m span railway viaducts

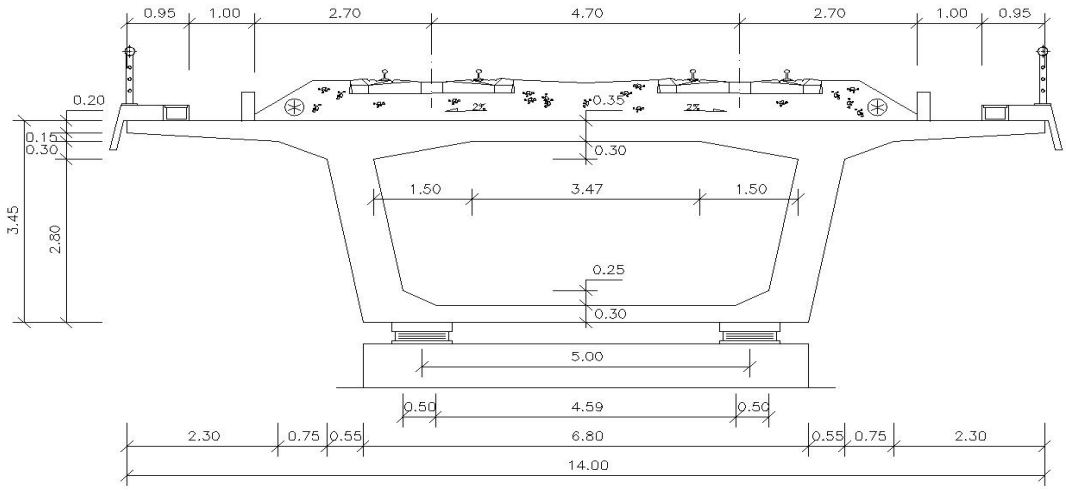

Fig. 5 Deck-section considered for the 60 m span railway viaducts

2.3 Cost function

The formulation seeks to find a pier that result in the lowest cost of the structure defined in Eq. (1), where p_i are the unit prices (Table 2) while m_i are the measurements of the units into which the construction of the RC pier is split. The total cost is the cost to minimize and is obtained adding all partial costs obtained by multiplying each measurement by its unit price. These unit prices were obtained from Spanish contractors of railway construction (Martínez *et al*. 2010, 2011) and include the price of materials (concrete and steel) and all the tasks required to build the pier. Note that the prices have been quite stable in the Spanish market where prices have not changed much for years due to keen contractor and subcontractor competition, compounded by the fact that the current financial crisis has affected public investments in infrastructure in Spain. The reinforcement price includes supply, bending, and assembly and built according to regulations; even blunt, tied and overlapping. The formwork price includes supply, laying with the necessary means, strip forms and cleanliness, even the proportional part of wedges, shoring and form-release agents. Concrete cost is variable and depends on the type of concrete and the pump necessary to place it. The unit concrete cost includes its production, transport, placing, vibration and cure. The excavation of the area included freeing, clearing the vegetation and excavation with mechanical machinery, enclosed extraction, load and transport to dump or to the place to fill. The fill is performed by material from the excavation or from another part of the construction site and is compacted in stages of thickness up to 25 cm using vibrant tray.

2.4 Problem constraints

The structural constraints are all the limit states with which the column and the foundation must comply in accordance to EHE (Ministerio de Fomento 2008) and Eurocode 2 (CEN 2004a)

Table 2 Basic prices of the cost function of the reported piers in Euros

Unit	Unit cost (€)
Kg of steel (B-500S)	0.73
m^2 of foundation formwork	18.00
m^2 of wall exterior formwork	48.19
m^2 of wall interior formwork	48.50
m^2 of sheet top end block formwork	120.48
m^3 of footing concrete (labour)	6.20
m^3 of wall concrete (labour)	6.50
m^3 of concrete pump rent	6.01
m^3 of concrete HA-25	45.24
m^3 of concrete HA-30	49.38
m^3 of concrete HA-35	53.90
m^3 of concrete HA-40	59.00
m^3 of concrete HA-45	63.80
m^3 of concrete HA-50	68.61
m^3 of earth removal	3.01
m^3 of earth fill-in	4.81

prescriptions. These constraints for bridge piers have been fully discussed in previous papers (Martínez *et al*. 2010, 2011), so they are briefly outlined here. Once the design variables defining a pier are set, then geometry, materials and passive reinforcement are fully defined. Reinforcing steel is checked against flexure, shear, cracking and fatigue, while the greatest amount of computational time required is buckling ULS. If one of the sections does not verify all conditions the column is unfeasible. Shear is checked firstly because its computational time is the lowest. As soon as it is detected that one condition does not verify, the column is unfeasible, in this way the algorithm does not lose time unnecessarily. Buckling and flexure are the following verifications. Buckling was checked by the stiffness method as reported by Manterola (2000). The method starts supposing an initial construction imperfection defined in Eurocode 2 (CEN 2004a), the deformed shape of the column is calculated using the stiffness method. With this deformed shape it is possible to calculate first and second-order bending moments to check flexure in every section of the column. In addition, it is possible to obtain the moment-curvature diagram to calculate the column deformation for the next iteration. This process is replicated until the difference between longitudinal and transverse deflections differs by less than 5% from the values of the previous iteration. Finally if all sections verify the checking, cracking and fatigue are tested. The integration of sections is performed with the Gauss-Legendre quadrature proposed by Bonet *et al*. (2004). With the appropriate numbers of Gauss, this numerical calculation method reaches the integral exact solution.

The design of the footing should involve the limit load of the soil and the soil/structure interaction during an earthquake analysis. The bearing capacity of footing depends on cohesion, overburden, and the weight of the soil. However, we have assumed that allowable stress acting on rock as well as that in the place of the structure is supposed that the earthquake acceleration is low enough to be considered. In this case, it is checked that the ground has sufficient bearing resistance to withstand the actions. For design purposes, it is customary to assume that the distribution of stresses under the footing is considered linear: a triangular distribution is used in case of lifting and a trapezoidal block otherwise. This is a satisfactory assumption at service-load levels and for footings on rock. Peak values can increase by 25% compared to the permissible ground stress and the smallest value has to be positive. The allowable stress design depends on the footing plan areas. Nevertheless, all footing plan areas are similar and are built in a solid rock, so allowable pressure is limited to 500 KPa in all foundations. Lower values of the allowable soil pressure (e.g.: 200-250 KPa) lead to pile foundation design in order to restrict economically the large size of the surface footing. Reinforcing steel is checked against flexure, shear, cracking and fatigue in the two directions.

In addition, the procedure checks all the constraints for minimum amounts of reinforcement due to flexural, shear and geometry as prescribed by Eurocode 2 and EHE (CEN 2004a, Ministerio de Fomento 2008). Other than the structural constraints, the problem includes implicit constraints regarding the geometry, the materials and the constructability of solutions. Among others, these implicit constraints contain the choice of a hollow section, the set of bar diameters, the reinforcement set up, the maximum and minimum thicknesses of the walls, etc.

2.5 Design representation space

The design variables $x_1, x_2, \ldots, x_n$ are numbers whose values can be varied without restriction to define a solution, while the parameters are all the magnitudes taken as fixed data. All variables and parameters are discrete since the final solution of the optimization process has to be construable.

Design variables define the geometry, the concrete type and the steel reinforcement in the different parts of the pier. The number of column variables depends on the height of the pier (Table 3), since the column is built in stages. Every stage is limited by two sections (Fig. 2). Stages measure 5.00 m in general. However, the top block measures 3.00 m and stage 1 of the column measures 2.00 m. In all footings the number of variables is 16. Consequently, the total number of variables of the piers is given in Table 3.

Among the geometrical variables of the column is the side width of the top section. This variable can vary from 1.00m to 5.00m in steps of 0.05m and it has to be larger than the dimension of the pot bearing plus 0.20m. Other geometrical variables are the frontal and side thicknesses of the hollow sections. Thicknesses can vary between 0.25m and 0.75m in steps of 0.025m. The thicknesses of each stage must be equal to or smaller than those of the stage underneath. Next column variables are the concrete qualities of the stages, which must decrease with the height. These qualities can vary between the HA-25 and the HA-50 considered by the structural code EHE (Ministerio de Fomento 2008), the number indicating the characteristic compressive cylinder strength at 28 days. Regarding to the steel reinforcement of the column, the longitudinal vertical reinforcement of the column is defined by the spacing and the diameter of the bars, which is different for the frontal and side walls and for the outer and inner faces. This means eight variables per stage. Nominal bar diameters considered are 12, 16, 20, 25 and 32mm and spacing varies from 0.10m to 0.30m in steps of 0.02m. The number and diameter of bars must be equal to or smaller than that of the stage bellow. The shear horizontal reinforcement accounts for three variables per hollow stage: the bar diameters in the frontal and side walls and the vertical spacing. The diameters considered are 12, 16 and 20mm and the spacing varies from 0.10 to 0.30m in steps of 0.025m. Finally, the reinforcement of the top stage of the pier is calculated and added to the measurement of passive reinforcement. Additionally, parallel walls have the same inclination and the internal walls have the same inclination that external walls, so all cross-sections of the column keep double symmetry.

There are 16 variables that define footing values. The first five ones are geometrical and define the total footing depth, the rectangular footing and the plinth plan dimensions. Plinth depth is equal to half the total depth of the footing. Footing depths vary between 1.00 and 5.00m in steps of 0.10m, and the plan dimensions of the footing measure between 8.00 and 25.00m in steps of 0.25m. The plan dimensions of the plinth range from 4.00 to 25.00m in steps of 0.25m. Another variable defines the type of concrete and the 10 remaining variables determine the cover and the footing and plinth reinforcement.

Table 3 Number of column, foundation and total variables

Column height (m)	Number of variables		
	Column	Foundation	Total
40	123	16	139
50	151	16	167
60	179	16	195
70	207	16	223
80	235	16	251
90	263	16	279
100	291	16	307

Table 4 Basic parameters of geometry and foundation of the pier

Parameter	Values
Transverse dimension of the pier	6.80m
Height of top end block	3.00m
Height of formwork stages	5.00m
Number of bearings	2
Spacing of bearings	5.00m
Earth fill density	20.00 kN/m^3
Permissible ground stress	500.00 kN/m^2

Table 5 Vertical reactions transmitted by the deck to the pier (kN)

Load combination	Horizontal span (m)					
	40		50		60	
	PU-1600	PF-1600	PU-2000	PF-2000	PU-2600	PF-2600
Permanent loads	7742	7742	10246	10246	13038	13038
Maximum load	14890	14890	19027	19027	23451	23451
Maximum torque	15106	8211	19300	10828	23783	13732
Minimum load	7059	7059	9391	9391	12012	12012

Table 6 Longitudinal friction force transmitted by the pot bearings to the pier (kN)

Column height (m)	Horizontal span (m)		
	40	50	60
40-50-70-80-90-100	774	1025	1304

Table 7 Transverse wind force transmitted by the deck to the pier (kN)

Column height (m)	Horizontal span (m)		
	40	50	60
40	809	1142	1515
50	849	1199	1591
60	883	1247	1654
70	912	1288	1709
80	938	1324	1757
90	960	1356	1799
100	981	1386	1838

Parameters in the formulation describe structural geometry, material properties, ground properties, applied loads, construction costs, available reinforcement sizes, partial safety factors and durability requirements (Tables 4 to 7). As mentioned above, the main geometric parameter is the different height of the piers (40, 50, 60, 70, 80, 90 and 100 m). Another geometric parameter is the dimension of the frontal side of the top cross-section that is 6.80m and is given by the soffit of the bridge decks. The side walls (Fig. 2) are vertical along the shaft and the frontal walls are inclined, with an inclination of 1/100 the two walls. We also introduce typical parameter values for the construction process, the parameters are the column height of the stages (5.00m) and the top height (3.00 m) and column bottom stages. Other parameters are the number, spacing and the type of bearings. It has been considered that both are pot bearings, one multidirectional and the other one unidirectional (i.e., it only allows the longitudinal movement). The actions and the ground properties parameters are: the density of the fill earth over the footing, the permissible ground stress depending on the plan footing, the reactions transmitted by the deck to the pier across the bearings and the rest of actions along the shaft, like the wind. Reinforcing parameters are the type of steel (B-500S) and the reinforcement in the lateral sides of the footing (Ø12/20). Finally, durability exposure conditions contemplate the different environmental conditions of the piers.

3. Optimization method

The original ant colony optimization (ACO) method was originally proposed by Dorigo *et al*. (1996) to solve several discrete optimization problems. ACO is an iterative distributed algorithm based on the collective behaviour of real ants in cooperating to find shortest paths to food. In nature, an individual ant is much unsophisticated insect, but an ant colony behaves as an intelligent system. The key reason lies in the interactions between large numbers of individual ants and their environment. When ants first leave the nest, they move in a random manner and deposit a constant amount of a chemical substance called pheromone. Therefore, the path of a second group of ants foraging for food will depend both on the pheromone trail left by the first stage ants as well as a random component. In addition, successive stages of ants accentuate the pheromone trail of previously explored paths or discover new and shorter paths, where the pheromone trail is quickly improved given that more ants follow the path in less time leaving additional pheromone. Evaporation causes longer paths where the pheromone over time as opposed to shorter paths where this substance is replaced faster. Consequently, the more ants take the short path, the more pheromone is deposited. Anyhow, the random component of the search guarantees the diversity of the search.

The application of the proposed ACO algorithm follows from Eqs. (4) to (7)

$$\Delta T(t,k,i,j) = \left(\frac{F_{\min}}{F(k)}\right)^{100} \tag{4}$$

$$\Delta T(t,i,j) = \sum_{k=1,H} \Delta T(t,k,i,j) \tag{5}$$

$$T(t,i,j) = e_v \cdot \Delta T(t,i,j) \cdot \left(\frac{F_{\min}}{F_{\min,t}}\right)^{100} \cdot T(t-1,i,j) + \left(\frac{F_{\min}}{F_{\min,t}}\right) \cdot \Delta T(t,i,j) \tag{6}$$

$$P(t,k,i,j) = \alpha(t) \cdot \frac{T(t,i,j)}{T(t,i)} + \beta(t) \cdot R \tag{7}$$

An ant is a solution in the ant colony optimization algorithm. Trial solutions are constructed incrementally as artificial ants move from one decision point to the next until all decisions points have been covered. Thus, the calculation process involves a number of stages with H ants generated in every stage. The total number of stages considered, t_{max}, is 100. The first stage generates H = 50 ants by randomly selecting the values of the variables. In the first stage, the system has no information so the ants find solutions in a random way. The cost of the lowest cost ant is called $F_{\min}$, which will be, in the remainder of this analysis, the lowest cost of all the ants generated throughout all the stages of the algorithm. With these solutions, we can calculate the pheromone trail increment left by a single ant, $\Delta T(t,k,i,j)$, by using Eq. (4), where $F(k)$ is the cost of the k ant; t is the number of stage; i is the number of variable; and j is the position in the list of possible values for the variable. Note that the exponent of 100 in the Eq. (4) is a coefficient of intensification such that low cost ants leave far more pheromone than do more expensive ants. (It should be note that other exponents were tentatively tried before the results reported in Section 4 and that the 100 value was maintained.) It then follows the calculation of the trace increment left by the entire set of ants of the stage, $\Delta T(t,i,j)$, which is given by adding in Eq. (5) the pheromone trails. That is, pheromone is updated after the completion of one stage. Then, Eq. (6) calculates the total trace at the end of stage t, $T(t,i,j)$, which depends both on the trace increment and on the total trace at the end of the previous stage. $F_{\min,t}$ is the lowest cost of the 50 ants generated in the current stage t. The formula also includes an evaporation coefficient e_v, which is taken as unity. Lastly, Eq. (7) indicates the probability of selecting the j position of the i variable, ant k and stage t. The expression includes the term $T(t,i)$, which is the addition of all the traces of all the positions of variable i after stage t. Once a stage has been completed, and H ants have been constructed, the pheromone trails are updated in a way that reinforces good solutions. It is worth noting the inclusion of two user-defined parameters, α and β, which specifies the impact of trace and random selection, respectively. R is a uniform random number between 0 and 1. The results in the next section include initial values for α and β of 0.9-0.1 for the column and 0.8-0.2 for the footing, so the trace left prevalence is more decisive than the random choice. Anyway, α and β are made to converge to 1 and 0 ($\alpha + \beta = 1$) in order to converge to full use of the trace search with no exploration (random) search. The convergence of α and β to 1 and 0, respectively, is linearly made with the number of stages, i.e., $\alpha = \alpha_o + (1-\alpha_o) \cdot t/t_{\max}$. Once we know the probability of each position j, the procedure generates ants by the typical roulette wheel selection, bearing in mind the high or low probability of choosing a position.

A number of runs of each algorithm were performed for statistical purposes given the random nature of the results. It was fixed using a Student's t-distribution and required that approximate 95% confidence interval of the population mean be estimated with an error less than 0.5% of the minor cost of the results in the first stage population. The estimated error is given by $t_{N-1}^{2.5} s/\sqrt{N}$, where $t_{N-1}^{2.5}$ is the Student's t-distribution coefficient, s is the standard deviation and N is the number of runs.

4. Numerical results

This section presents the results obtained in the 21 piers with rectangular hollow sections typically used in railway construction of prestressed concrete viaducts. Figs. 6 to 18 summarize the main results of the piers analyzed. The algorithm was programmed in Fortran Compaq Visual Professional Edition 6.6.0. Computer runs were performed in a conventional PC computer with an Intel Corel 2 CPU of 3.00 GHz and 2 GB of RAM.

Figs. 6 to 12 refer to geometry, steel reinforcement and concrete in the different columns. Fig. 6 depicts the column width at the bottom section versus the column height, which varies from a minimum of 3.20 m for the 40 m height pier and 40 m span viaduct (least loaded pier henceforth) to a maximum of 6.90 m for the 100 m height pier and 60 m span viaduct (most loaded pier henceforth). The frontal walls are inclined with an inclination of 1/100 in the two walls, so the column widths at the top section are 2.40 m (3.20-2*40/100) for the least loaded pier and 4.90 m (6.90-2*100/100) for the most loaded pier. Fig. 7 gives the measurement of concrete in the column. This measurement varies from a minimum of 232.59 m^3 for the least loaded pier to a maximum of 814.69 m^3 for the most loaded pier.

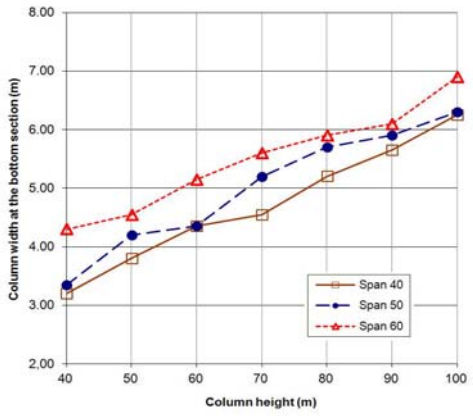

Fig. 6 Column width at the bottom section

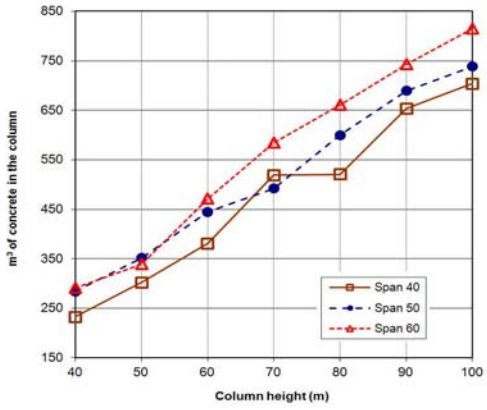

Fig. 7 Measurement of concrete in the column

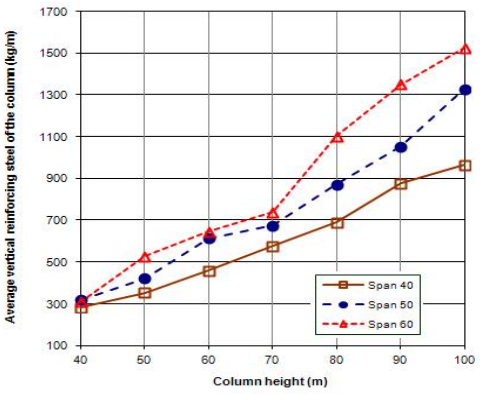

Fig. 8 Average vertical reinforcing steel of the column

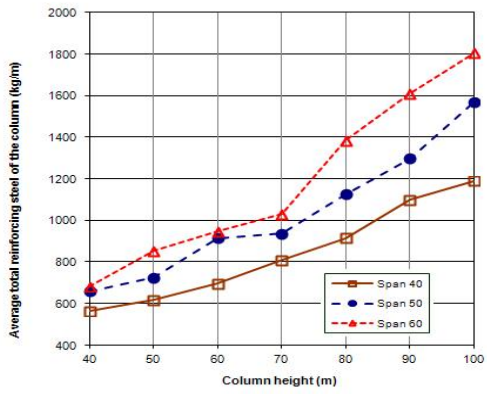

Fig. 9 Average total reinforcing steel of the column

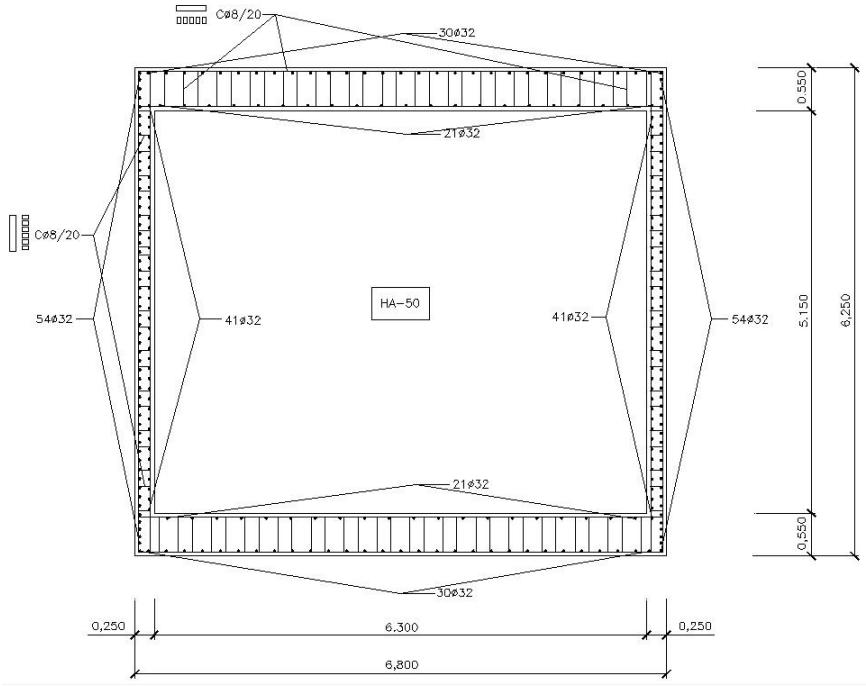

Fig. 10 Bottom cross-section for the 40 m span viaduct and 100 m pier height

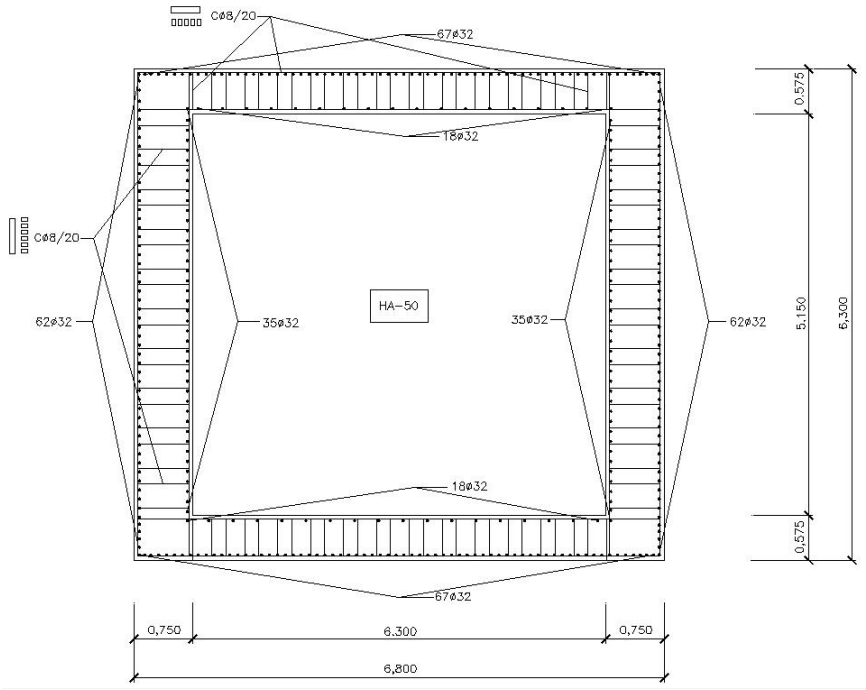

Fig. 11 Bottom cross-section for the 50 m span viaduct and 100 m pier height

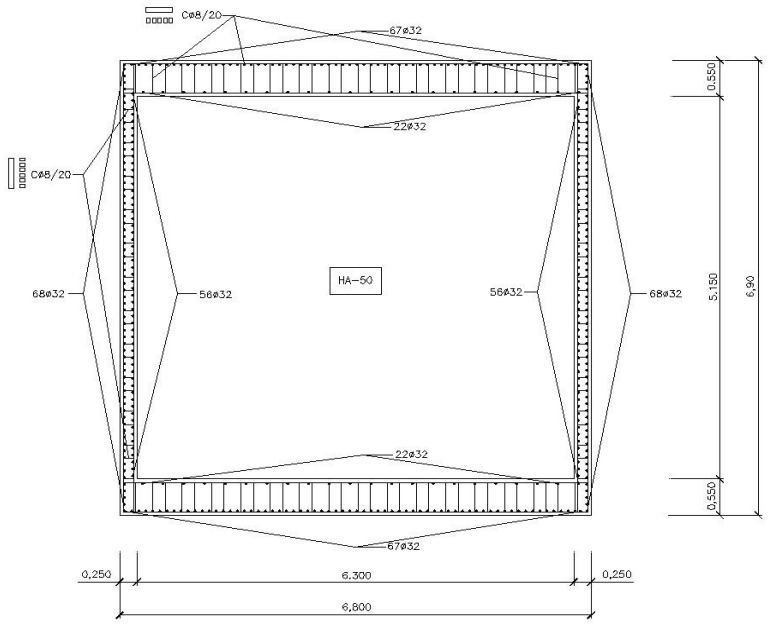

Fig. 12 Bottom cross-section for the 60 m span viaduct and 100 m pier height

Fig. 8 details the measurement of the vertical reinforcement steel in the column per unit height and, thus, it can be used to total the amount of vertical reinforcing steel in the column. Vertical reinforcement in the column varies from a minimum of 280.76 kg/m to a maximum of 1526.83 kg/m. Moreover, Fig. 9 gives the total reinforcing steel in the column per unit height. Total reinforcement accounts for the vertical, the shear and the top block reinforcement. Total reinforcement in the column varies from a minimum of 563.03 kg/m to a maximum of 1804.41 kg/m. Figs. 10 to 12 give three examples of detailed design of the bottom cross-section. They correspond to the 100 m height and 40 m, 50 m and 60 m span lengths, i.e. the tallest 3 piers of the study. Regarding the footing, Figs. 13 to 15 detail their main characteristics. Fig. 13 depicts the footing's plan area versus the column height, which varies from a minimum of 105.75 m^2 for the least loaded pier to 399.75 m^2 for the most loaded pier. Fig. 14 gives the measurement of concrete in the footing. This measurement varies from a minimum of 243.23 m^3 for the least loaded pier to a maximum of 1817.47 m^3 for the most loaded pier. Regarding reinforcing steel in the footing, Fig. 15 shows a variation from a minimum of 12947.16 kg to a maximum of 91596.73 kg. Finally, Figs. 16 to 18 aggregate measurement and cost of the 21 piers. Figs. 16 and 17 detail measurements of steel and concrete per unit height in the whole pier, which vary from a minimum of 886.71 kg/m and 11.90 m^3/m to a maximum of 2720.38 kg/m and 26.32 m^3/m. These figures show the upward trend with the pier height and the span length. Fig. 18 details the average cost of the piers. We observe that the trend of Fig. 18 is similar to the trend of Figs. 16 and 17 because the total cost is directly related to the material measurements. In addition, it has been found that buckling and combination of compression and bending are the failure modes of columns, whereas bending and shear are failure modes of footing, once size is adjusted according to geotechnical properties of the ground. The average cost of the piers varies from a minimum of 3221.42 €/m for the least loaded pier to a maximum of 6206.38 €/m for the most loaded pier, so the total cost of piers vary from 128,856.80 € to 620,638.00 €.

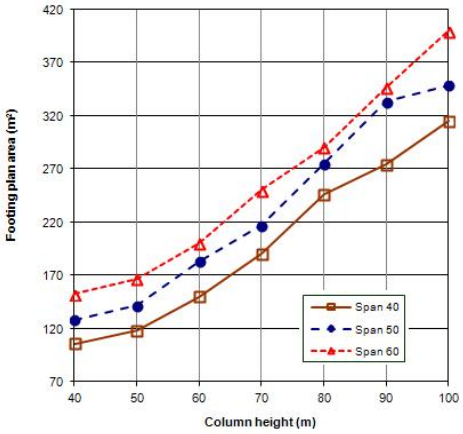

Fig. 13 Footing plan area versus column height

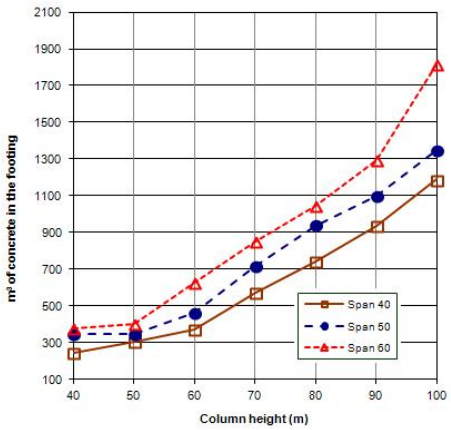

Fig. 14 Measurement of concrete in the footing

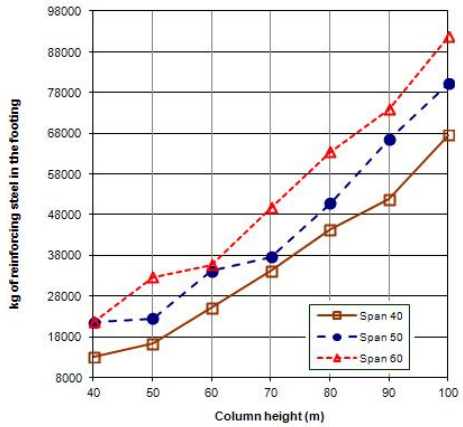

Fig. 15 Total reinforcing steel in the footing

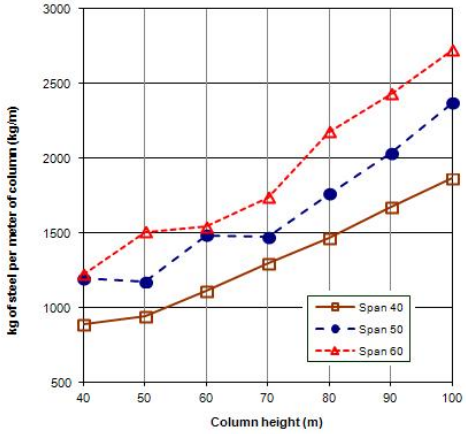

Fig. 16 Total measurement of steel in the pier

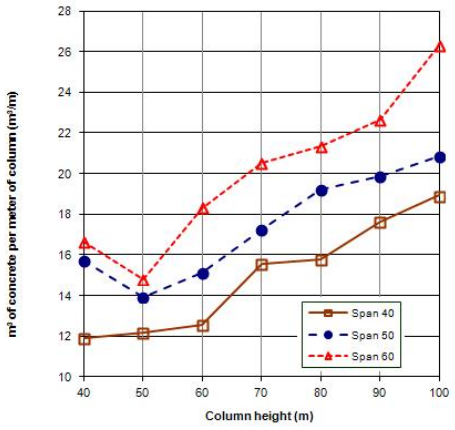

Fig. 17 Total measurement of concrete in the pier

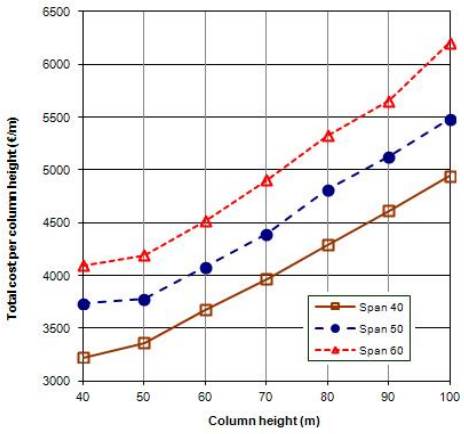

Fig. 18 Total pier's cost per unit column hight

5. Conclusions

Twenty one different types of rectangular hollow piers have been studied with column heights of 40, 50, 60, 70, 80, 90 and 100 meters for prestressed railway continuous bridges with center span lengths of 40, 50 and 60 m. The optimization procedure used in the present study to minimize the objective function is a variant of the ant colony optimization described in Section 3 and requires the definition of the initial values for α and β in Eq. (7), the number of ants (solutions) in every stage and the total number of stages. The results include initial values for α and β of 0.9-0.1 for the column and 0.8-0.2 for the footing. In any case, α and β are made to converge to 1 and 0 and $\alpha + \beta = 1$ during the optimization process. The number of ants in every stage is 50, that number is the same as the solutions for the variant of the ant colony optimization used in this work. The total number of stages is 100. Three main conclusions may be drawn from this study. First, RC bridge piers can potentially use heuristic algorithms for the advanced automatic design of real concrete structures. It is essential to note that the present model eliminates the need for experience-based rules of design. Second, the total cost, the steel cost and the concrete cost may be estimated with a high degree of accuracy and is obtained adding all partial costs obtained by multiplying each measurement by its unit price. Finally, the data figures may be used for the preliminary optimum geometry design.

Acknowledgments

This study was funded by the Spanish Ministry of Science and Innovation (Research Project BIA2011-23602).

References

Adeli, H. and Sarma, K.C. (2006), *Cost Optimization of Structures*, John Wiley & Sons, Chichester, UK.

Awad, Z.K. and Yusaf, T. (2012), "Fibre composite railway sleeper design by using FE approach and optimization techniques", *Struct. Eng. Mech.*, **41**(2), 231-242.

Balling, R.J. and Yao, X. (1997), "Optimization of reinforced concrete frames", *J. Struct. Eng.*, *ASCE*, **123**(2), 193-202.

Bonet, J.L., Romero, M.L., Miguel, P.F. and Fernández, M.A. (2004), "A fast stress integration algorithm for reinforced concrete sections with axial loads and biaxial bending", *Comput. Struct.*, **82**(2-3), 213-225.

Carbonell, A., González-Vidosa, F. and Yepes, V. (2011), "Design of reinforced concrete road vault underpasses by heuristic optimization", *Adv. Eng. Softw.*, **42**(4), 151-159.

CEN (2003), *EN 1991-2: Eurocode 1. Basis of Design and Actions on Structures. Part 2: Traffic Loads on Bridges*, Comité Européen de Normalisation, Brussels, Belgium.

CEN (2004a), *EN 1992-1-1: Eurocode 2. Design of Concrete Structures - Part 1-1: General Rules and Rules for Building*, Comité Européen de Normalisation, Brussels, Belgium.

CEN (2004b), *EN 1998-1: Eurocode 8. Design of Structures for Earthquake Resistance - Part 1: General Rules, Seismic Actions and Rules for Buildings.* Comité Européen de Normalisation, Brussels, Belgium.

Coello, C.A., Christiansen, A.D. and Santos, F. (1997), "A simple genetic algorithm for the design of reinforced concrete beams", *Eng. Comput.*, **13**(4), 185-196.

Cohn, M.Z. and Dinovitzer, A.S. (1994), "Application of structural optimization", *J. Struct. Eng.*, *ASCE*, **120**(2), 617-649.

Dorigo, M., Maniezzo, V. and Colorni, A. (1996), "The ant system: optimization by a colony of cooperating

agents", *IEEE Trans. Syst. Man Cybern. Part B*, **26**(1), 29-41.
Holland, J.H. (1975), *Adaptation in Natural and Artificial systems*, University of Michigan Press, Ann Arbor, USA.
Kaveh, A. and Sabzi, O. (2011), "A comparative study of two meta-heuristic algorithms for optimum design of reinforced concrete frames", *Int. J. Civ. Eng.*, **9**(3), 193-206.
Kennedy, J. and Eberhart, R. (1995), "Particle Swarm Optimization", *IEEE International Conference on Neural Networks*, IEEE Service Center, Piscataway, Perth, Australia, 1942-1948.
Khajehzadeh, M., Taha, M.R., El-Shafie, A. and Eslami, M. (2011), "Modified particle swarm optimization for optimum design of spread footing and retaining wall", *J. Zhejiang Univ.-SCI A*, **12**(6), 415-427.
Kicinger, R., Arciszewski, T. and De Jong, K. (2005), "Evolutionary computation and structural design: A survey of the state-of-the-art", *Comput. Struct.,* **83**(23-24), 1943-1978.
Kirkpatrick, S., Gelatt, C.D. and Vecchi, M.P. (1983), "Optimization by simulated annealing", *Science*, **220**, 671-680.
Lee, E.H. and Park, J. (2011), "Structural design using topology and shape optimization", *Struct. Eng. Mech*., **38**(4), 517-527.
Lee, K.S. and Geem, Z. (2004), "A new structural optimization method based on the harmony search algorithm", *Comput. Struct.*, **82**(9-10), 781-798.
Li, G., Lu, H. and Liu, X. (2010), "A hybrid simulated annealing and optimality criteria method for optimum design of RC buildings", *Struct. Eng. Mech*., **35**(1), 19-35.
Liao, T.W., Egbelu, P.J., Sarker, B.R. and Leu, S.S. (2011), "Metaheuristics for project and construction management – A state-of-the-art review", *Autom. Constr.***, 20**(5), 491-505.
Lignola, G.P., Prota, A., Manfredi, G. and Cosenza, E. (2007), "Deformability of reinforced concrete hollow columns confined with CFRP", *ACI Struct. J.*, **104**(5), 629-637.
Manterola, J. (2000), *Bridges: volume IV*. ETS Ingenieros Caminos, Madrid, Spain. (in Spanish)
Martí, J.V., González-Vidosa, F., Yepes, V. and Alcalá, J. (2013), "Design of prestressed concrete precast road bridges with hybrid simulated annealing", *Eng. Struct.*, **48**, 342-352.
Martínez, F.J., González-Vidosa, F., Hospitaler, A. and Alcalá, J. (2011), "Design of tall bridge piers by ant colony optimization", *Eng. Struct.*, **33**(8), 2320-2329.
Martínez, F.J., González-Vidosa, F., Hospitaler, A. and Yepes, V. (2010), "Heuristic optimization of RC bridge piers with rectangular hollow sections", *Comput. Struct.*, **88**(5-6), 375-386.
Martínez, P., Martí, P. and Querin, O.M. (2007), "Growth method for size, topology, and geometry optimization of truss structures", *Struct. Multidisc. Optim.*, **33**(1)**,** 13-26.
Ministerio de Fomento (2007). *IAPF: Code for Actions for the Design of Railway Bridges.* Ministerio de Fomento, Madrid, Spain. (in Spanish)
Ministerio de Fomento (2008), *EHE: Code of Structural Concrete*, Ministerio de Fomento, Madrid, Spain. (in Spanish)
Payá, I., Yepes, V., González-Vidosa, F. and Hospitaler, A. (2008), "Multiobjective optimization of concrete frames by simulated annealing", *Comput.-Aided Civil Infrastruct. Eng.***, 23**(8), 596-610.
Payá-Zaforteza, I., Yepes, V., Hospitaler, A. and González-Vidosa, F. (2009), "CO_2 efficient design of reinforced concrete building frames", *Eng. Struct.*, **31**(7), 1501-1508.
Payá-Zaforteza, I., Yepes, V., Hospitaler, A. and González-Vidosa, F., (2010), "On the Weibull cost estimation of building frames designed by simulated annealing", *Meccanica*, **45**(5), 693-704.
Perea, C., Alcalá, J., Yepes, V., González-Vidosa, F. and Hospitaler, A. (2008), "Design of reinforced concrete bridge frames by heuristic optimization", *Adv. Eng. Softw.*, **39**(8), 676-688.
Perea, C., Yepes, V., Alcalá, J., Hospitaler, A. and González-Vidosa, F. (2010), "A parametric study of optimum road frame bridges by threshold acceptance", *Indian J. Eng. Mater. S.*, **17**(6), 427-437.
Yepes, V., Alcalá, J., Perea, C. and González-Vidosa, F. (2008), "A parametric study of earth-retaining walls by simulated annealing", *Eng. Struct.*, **30**(3), 821-830.
Yepes, V., González-Vidosa, F., Alcalá, J. and Villalba, P. (2012), "CO_2-Optimization design of reinforced concrete retaining walls based on a VNS-threshold acceptance strategy", *J. Comp. Civil Eng*., *ASCE*, **26**(3), 378-386.